Published in final edited form as:
J Neurosci Methods. 2009 September 15; 182(2): 236–243. doi:10.1016/j.jneumeth.2009.06.015.

Detection of Reduced GABA Synthesis Following Inhibition of GABA Transaminase Using in Vivo Magnetic Resonance Signal of [^{13}C]GABA C1

Jehoon Yang[1,2], **Christopher Johnson**[1], and **Jun Shen**[1]

[1] National Institute of Mental Health Intramural Research Program, Bethesda, Maryland, USA

[2] Samsung Biomedical Research Institute, Seoul, Korea

Abstract

Previous in vivo magnetic resonance spectroscopy (MRS) studies of gamma-aminobutyric acid (GABA) synthesis have relied on ^{13}C label incorporation into GABA C2 from [1-^{13}C] or [1,6-$^{13}C_2$]glucose. In this study, the [^{13}C]GABA C1 signal at 182.3 ppm in the carboxylic/amide spectral region of localized in vivo ^{13}C spectra was detected. GABA-transaminase of rat brain was inhibited by administration of gabaculine after pre-labeling of GABA C1 and its metabolic precursors with exogenous [2,5-$^{13}C_2$]glucose. A subsequent isotope chase experiment was performed by infusing unlabeled glucose, which revealed a markedly slow change in the labeling of GABA C1 accompanying the blockade of the GABA shunt. This slow labeling of GABA at elevated GABA concentration was attributed to the relatively small intercompartmental GABA-glutamine cycling flux that constitutes the main route of ^{13}C label loss during the isotope chase. Because this study showed that using low RF power broadband stochastic proton decoupling is feasible at very high field strength, it has important implications for the development of carboxylic/amide ^{13}C MRS methods to study brain metabolism and neurotransmission in human subjects at high magnetic fields.

Keywords

GABA; ^{13}C; magnetic resonance spectroscopy; proton decoupling; glucose metabolism

Introduction

Gamma-aminobutyric acid (GABA), like glutamate and aspartate, differs from other central nervous system (CNS) transmitters in that its metabolism proceeds directly through substances

Address correspondence to: Jun Shen, PhD, Bldg. 10, Rm. 2D51A, 9000 Rockville Pike, Bethesda, MD 20892, Tel: 301-451-3408, Fax: 301-480-2397, Email: shenj@intra.nimh.nih.gov.
Jehoon Yang, Ph. D., Molecular Imaging Branch, National Institute of Mental Health, Bldg. 10, Rm. 2D50, 9000 Rockville Pike, Bethesda, MD 20892-1527
Samsung Biomedical Research Institute, 50 Ilwon-dong, Kangnam-Gu, Seoul, Korea, Tel.: 010 5572 7247, Email: jehoon.yang@sbri.co.kr
Christopher Johnson, B. S., Molecular Imaging Branch, National Institute of Mental Health, Bldg. 10, Rm. 2D51A, 9000 Rockville Pike, Bethesda, MD 20892-1527, Tel.: (301) 402-6695, Fax: (301) 480-2395, Email: johnsonchri@mail.nih.gov
Jun Shen, Ph. D., Molecular Imaging Branch, National Institute of Mental Health, Bldg. 10, Rm. 2D51A, 9000 Rockville Pike, Bethesda, MD 20892-1527, Tel.: (301) 451-3408, Fax: (301) 480-2397, Email: shenj@intra.nimh.nih.gov

that are important intermediates in the tricarboxylic acid cycle. The synthesis of GABA in the CNS takes place primarily in GABAergic neurons via the action of glutamic acid decarboxylase (GAD65 and GAD67) (Hertz 1979, Tapia, 1983). Most GAD65 is localized in presynaptic GABAergic nerve terminals and is thought to provide GABA for neurotransmitter release. GAD67 is present in both nerve terminals and cell bodies, where it may serve the nonsynaptic intracellular GABA pool (Kaufman et al, 1991; Martin and Rimvall, 1993). In addition, GAD is also expressed in certain glutamatergic neurons (Sloviter et al, 1996). In contrast to the presence of GAD in neurons, an overwhelming body of evidence indicates that this enzyme is absent in astrocytes (Hertz 1979). GABA is catabolized by GABA transaminase, which is expressed in both neurons and astrocytes (Tunnicliff, 1986). Brain GABA concentrations increase significantly after inhibition of GABA-T (e.g., by gabaculine or vigabatrin) (e.g., Behar and Boehm, 1994; Manor et al, 1996). Elevated GABA levels due to GABA-transaminase inhibition have been shown to originate mainly in neurons (Neal and Shah, 1990). Both acute and chronic GABA-transaminase inhibition methods have proved to be very useful in elucidating the metabolic fluxes associated with GABA metabolism and neurotransmission (e.g., Manor et al, 1996; de Graaf et al, 2006; Patel et al, 2006; Yang et al, 2005; 2007).

The rate of GABA synthesis can be directly measured using infusion of ^{14}C-labeled glucose to determine label incorporation into glutamate and, subsequently, GABA. In addition, ^{15}N-based MRS methods can also be used to study the synthesis of glutamine as a metabolic precursor of GABA (Kanamori and Ross, 1995, 1997; Kanamori et al, 1997). GABA synthesis from glucose increases in the presence of high K^+ concentrations, electrical stimulation, or bicuculline-induced seizures ex vivo or in vivo (de Belleroche and Bradford, 1972; Chapman and Evans, 1983). GABA synthesis or turnover is also regulated by changes in its receptor activity (Lindgren 1987). For example, potentiation of postsynaptic GABAergic transmission by benzodiazepines or hypoglycemia down-regulates GABA turnover (Paulsen and Fonnum, 1987).

In addition to radioactive isotope methods, ^{13}C nuclear magnetic resonance (NMR)-based techniques have been used to measure GABA synthesis rate ex vivo and in vivo (e.g., Manor et al, 1996; Hassel et al, 1998; Yang et al, 2005; Yang and Shen, 2005; de Graaf et al, 2006). Essentially, all current ^{13}C NMR-based methods for studying GABA synthesis use [1-^{13}C] or [1,6-$^{13}C_2$]glucose infusion and detection of ^{13}C-label incorporation into GABA C2. When [2-^{13}C]glucose, [2,5-$^{13}C_2$]glucose or [1-^{13}C]acetate is infused, the ^{13}C labels are primarily incorporated into carboxylic and/or amide carbons of glutamate, glutamine, and aspartate (Badar-Goeffer et al, 1990; Kanamori et al, 2001; Bluml et al, 2002). We recently showed that it is possible to detect ^{13}C label incorporation into glutamate, glutamine, aspartate, N-acetylaspartate, bicarbonate, and GABA in the carboxylic/amide spectral region in vivo from infused exogenous [2-^{13}C]glucose using low radiofrequency power for proton decoupling (Li et al, 2007). Extension of this strategy to human studies has been proved to be very successful (Li et al, 2008, 2009; Sailasuta et al, 2008, 2009).

C2 and C5 carbons of glucose are incorporated into the C1 carbon of GABA in the carboxylic/amide spectral region (see Figure 1). In contrast to the commonly used aliphatic region (e.g., Shen et al, 1999;Li et al, 2005;Xu and Shen, 2006), detecting ^{13}C signals derived from [2-^{13}C] or [2,5-$^{13}C_2$]glucose in vivo in the carboxylic/amide region is free of spectral interference from subcutaneous lipid signals. One of the advantages of using the carboxylic/amide region is that it may make parallel imaging-based techniques directly applicable to in vivo ^{13}C MRS of brain because, without interference from subcutaneous lipid signals, carboxylic/amide ^{13}C signals can be localized using phased array coils and/or phase encoding gradients without resorting to techniques such as PRESS, STEAM, ISIS or outer volume suppression. Because the required overall decoupling power is very low, whole brain proton

decoupling of human subjects could be performed using stochastic decoupling schemes (Li et al, 2008).

To further extend the work described above, we attempted to study GABA synthesis and the effect of GABA transaminase inhibition in vivo in the rat brain at high magnetic fields. This study is the first to report in vivo detection of GABA synthesis based on the labeling of cerebral GABA C1. We found that the carboxylic ^{13}C signal of GABA C1 at 182.3 ppm was spectrally resolved from the neighboring glutamate C5 signal at 182.0 ppm in the rat brain in vivo at the high field strength of 11.7 Tesla; all detected metabolite carboxylic/amide signals were free from any interference from subcutaneous lipids. The effect of acute GABA transaminase inhibition was detected in vivo by following the kinetics of ^{13}C label incorporation into GABA C1. The use of isotope chase revealed a markedly reduced GABA synthesis following GABA-transaminase inhibition by gabaculine. Finally, this study also showed that low power broadband stochastic proton decoupling is feasible even at very high field strength, providing the impetus for developing carboxylic/amide ^{13}C MRS methods to study brain metabolism and neurotransmission in human subjects at high magnetic fields (e.g., 7 or 11.7 Tesla).

Materials and Methods

MR hardware

All experiments were performed on a Bruker AVANCE spectrometer (Bruker Biospin, Billerica, MA) interfaced to an 11.7 Tesla 89-mm bore vertical magnet (Magnex Scientific, Abingdon, UK) located in an unshielded room. The spectrometer is equipped with a 57-mm i.d. gradient (Mini 0.5, Bruker Biospin, Billerica, MA, with a maximum gradient strength of 3.0 G/mm and a rise time of 100 μs) for studying young adult rats in vivo. The deuterium lock Z_0 coil was used to compensate for the zero-order eddy current resulting from switching gradients. The first order eddy current was compensated for by the use of pre-emphasis with three time constants. No significant cross-axis pre-emphasis terms were found after switching off a 50% 500 ms test gradient applied to each individual gradient axis.

A home-built integrated RF surface coils/head holder system mounted on a half-cylindrical plastic cradle was used for the study. The ^{13}C and ^{1}H RF coils were coplanar and made of single-sided printed circuit board. The inner loop of the RF assembly was the ^{13}C coil with an inner diameter and conductor width of 10.8 mm and 4.3 mm, respectively. The outer loop was the ^{1}H coil with an inner diameter and conductor width of 23.6 mm and 5.4 mm, respectively. To provide shielding against ambient RF noise, the main body of the RF probe/animal handling system was built using an aluminum tube with an outer diameter of 56.6 mm. The lower end of the integrated RF surface coils/head holder system was an aluminum interface box for connecting RF cables, ventilation tubes, rectal thermal probe, and catheters (Li et al, 2005). The RF probe/animal handling system also provided rat head fixation and body support, and allowed maintenance of normal physiology over prolonged periods despite the increased cardiac load and blood draining associated with vertically positioned rats (Li et al, 2005). The animal handling system was mechanically interfaced to the magnet using an adaptor ring that allows vertical and angular positional adjustments. Commercial broadband low-pass and high-pass filters (Bruker Biospin, Billerica, MA) were inserted before the preamplifiers. No noise injection was found in the ^{13}C channel from the environment or due to proton decoupling.

Animal preparation

Male Sprague-Dawley rats (Taconic, Germantown, NY, USA; 167–202 g, n = 5) fasted for 24 hours with free access to drinking water were studied. “Principles of laboratory animal care” (NIH publication No. 86-23, revised 1996) were followed and the animal study protocol was approved by the National Institute of Mental Health Animal Care and Use Committee.

The animals were orally intubated and ventilated with a mixture of 70% N_2O/30% O_2 and 1.5% isoflurane. The left femoral artery was cannulated where plasma samples were periodically withdrawn to monitor arterial blood pressure, as well as arterial blood gases, pH, and plasma glucose concentrations using a blood analyzer (Bayer Rapidlab 860, East Walpole, MA). The left femoral vein was cannulated for infusion of [2,5-$^{13}C_2$]glucose (99% enrichment, Cambridge Isotope Labs, Andover, MA, 0.75 M) with an initial bolus of 113 mg/kg/min followed by infusion at a reduced rate that was adjusted over a small range to maintain constant plasma glucose levels. The [2,5-$^{13}C_2$]glucose infusion protocol rapidly raised plasma glucose concentrations to ~19.8 mM and maintained them there. Rectal temperature was maintained at ~37.5 °C using an external pump for water circulation (BayVoltex, Modesto, CA). Normal arterial blood physiological parameters were maintained by small adjustments of respiration rate and volume (pH = 7.38 ± 0.03, pCO_2 = 41 ± 5 mmHg, pO_2 = 125 ± 22 mmHg, mean arterial blood pressure > 100 mmHg with few exceptions). End-tidal CO_2, tidal pressure of ventilation, and heart rate were also monitored. Animals received gabaculine treatment (100 mg/kg, 0.6 cc, i.v.; BIOMOL Research Laboratories, Plymouth Meeting, PA) 2.5 hours after the start of the [2,5-$^{13}C_2$]glucose infusion. Two hours after gabaculine administration, the infusate was switched to natural abundance glucose (Sigma-Aldrich, St. Louis, MO). The concentration and the maintenance infusion rate for natural abundance glucose were the same as [2,5-$^{13}C_2$]glucose. The total duration of isotope chase was 4.4 hours.

In vivo MRS

Three-slice (coronal, horizontal, and sagittal) scout RARE images (FOV = 2.5 cm, slice thickness = 1 mm, TR/TE = 200/15 ms, rare factor = 8, 128 × 128 data matrix) were acquired first for positioning the RF probe/animal handling system inside the Bruker Mini 0.5 gradient insert. After positioning, the gradient isocenter was 0 – 1 mm posterior to bregma based on separate calibrations. A ~8.5 × 6 × 8.5 mm^3 spectroscopy voxel was placed at the gradient isocenter along the brain midline. The rat brain was shimmed as described previously using FASTMAP/FLATNESS methods (Chen 2004 and references therein). A train of non-selective hard pulses with a nominal flip angle of 180° spaced at 100 ms apart was used to generate broadband $^1H \rightarrow ^{13}C$ heteronuclear Overhauser enhancement. Direct three-dimensional spatial localization of ^{13}C spins in the carboxylic/amide region used a 0.75 ms adiabatic half-passage pulse, followed by three pairs of hyperbolic secant pulses (one pair per dimension, 2-ms per pulse, with phase factor = 5 and truncation level = 1%, TR/TE = 20000/18 ms) as described previously in the context of localized proton observation and ^{13}C editing (Slotboom and Bovee, 1995). The ^{13}C 180° pulses also refocused the long-range heteronuclear ^1H-^{13}C couplings during TE. No additional outer volume suppression schemes were necessary. Spectral width was set to 10 kHz with a data sampling time of 204.8 ms. During the data sampling time, ^1H decoupling was applied, which uses a pseudo noise (stochastic) decoupling scheme with constant γB_2 amplitude and randomly inverted phases (Ernst, 1966; Li et al, 2007) and a repetition unit of 0.2–0.4 ms. The pseudo noise decoupling scheme allowed effective broadband proton decoupling at 11.7 Tesla with a TR-averaged forward decoupling power at or above 5 mW, corresponding to a γB_2 of ~250 Hz calibrated at the center of the selected spectroscopy voxel. For each data block, 30 scans were acquired. After acquisition of each data block, a fixed two minute interval was allocated for re-shimming to maintain optimal B_0 homogeneity during a total of 6.5 hours of GABA-transaminase inhibition. Prior to Fourier transform, the time-domain data were zero-padded to 16 K. gb = 0.06, lb = −1. The ^{13}C signals in the carboxylic/amide region were analyzed using Bruker Biospin XWINNMR software (Bruker Biospin, Billerica, MA). The ^{13}C carrier frequency was placed around 180.4 ppm.

Brain and blood extracts

After in vivo MRS data acquisition of gabaculine-treated rats infused with [2,5-$^{13}C_2$]glucose and unlabeled glucose, the rats were euthanized using a microwave fixation device (Model

TNW-6402C, Muromachi Kikai Co., Tokyo, Japan, 5 kW, 1.5 sec). Subsequently, the rat heads (n = 5) were frozen in liquid nitrogen. Brain tissues corresponding to the spectroscopy voxel were removed, weighed, and subsequently extracted using perchloric acid (12% perchloric acid solution, 3–4 mL/g of sample) as described previously (Yang and Shen, 2005). Following centrifugation, the supernatants were neutralized using potassium hydroxide, re-centrifugated, and lyophilized repeatedly to remove residual water. The powder samples were then dissolved in D_2O. 3-(Trimethylsilyl) propionic-2,2,3,3-d_4 acid (TSP-d_4) was added as a chemical shift reference standard. The ^1H spectra of brain perchloric acid extracts in D_2O were acquired using a Bruker 2.5-mm broadband inverse probe without ^{13}C decoupling. The GABA H2 signals at 2.30 ppm were used to quantify [^{13}C]GABA C1. Due to the presence of ^{13}C label at GABA C1, the GABA H2 protons attached to [^{13}C]GABA C1 have a quartet spectral pattern when proton decoupling is turned off due to additional splitting by the two-bond scalar coupling between GABA C1 and GABA H2 ($^2J_{CH}$ = 7.3 Hz). The GABA H2 quartet originated from [^{13}C]GABA C1 was spectrally resolved from the GABA H2 triplet originated from [^{12}C] GABA C1. The integrated area of the GABA H2 quartet originated from [^{13}C]GABA C1 was quantified using the integrated area of the total creatine methyl proton singlet signal at 3.02 ppm as an internal standard. The concentration of total creatine, which is known to be unchanged due to GABA transaminase inhibition (Manor et al, 1996; Yang and Shen, 2005), was 8.5 μmol/g based on our previous work (Yang et al, 2005b). The concentration of [^{13}C] GABA C1 at the end point of the isotope chase experiment was then used to determine the concentration of [^{13}C]GABA C1, [^{13}C]glutamate C5, and [^{13}C]glutamine C5 in vivo.

The plasma protein component was denatured and precipitated using methanol (water:methanol = 1:4). After centrifugation to pellet the protein, the supernatant was transferred to a glass vial and the solvent was removed under vacuum. The residue was re-dissolved with 2% hydroxylamine in dry pyridine and incubated for 1 hour followed by an additional 30 minutes in the presence of acetic anhydride. The resulting aldonitrile penta-acetate derivative of glucose was analyzed by gas chromatography/electron impact-mass spectrometry (GC/EI-MS) operating in single ion monitoring (SIM) mode. The signal was recorded for characteristic ions of penta-O-acetyl-gluconitrile (314 m/z) and penta-O-acetyl-(2,5^{13}C)-gluconitrile (316 m/z), representing a loss of 73 m/z from the molecular ions. The fractional enrichment of [2,5-$^{13}C_2$]glucose was determined by measuring the peak area ratio of 316 m/z to the sum of 314 m/z and 316 m/z from the extracted ion chromatogram. A calibration curve of [2,5-$^{13}C_2$]glucose fractional enrichment versus area ratio was generated using known mixtures of [2,5-$^{13}C_2$]glucose and unlabeled glucose. The linear range for this method was 0–100% [2,5-$^{13}C_2$]glucose fractional enrichment with a lower limit of quantitation of 0.5% as determined empirically.

Results

Highly reproducible in vivo spectra were obtained of the carboxylic/amide spectral region measured from the rat brain at 11.7 Tesla after infusion of [2,5-$^{13}C_2$]glucose. Typical in vivo ^{13}C spectra acquired during acute GABA-transaminase inhibition and continuous infusion of [2,5-$^{13}C_2$]glucose are shown in Figure 2, with each spectrum corresponding to 30 averages. Signals were detected in the following frequencies: glutamate C5 at 180.2 ppm, glutamine C5 at 178.5 ppm, GABA C1 at 182.3 ppm, aspartate C4 at 178.3 ppm, glutamate C1 at 175.4 ppm, glutamine C1 at 174.9 ppm, aspartate C1 at 175.0 ppm, and N-acetylaspartate C5 at 174.3 ppm (Fig. 1). N-acetylaspartate C1 signals at 179.6 ppm and C4 signals at 179.4 ppm could also be seen after more signal averaging. Lipid carboxylic signals at 172.5 ppm (Li et al, 2008) were completely suppressed by the PRESS-type spatial localization employed here, although neither outer volume suppression nor retraction of the scalp under the surface coil was performed. No other signals in the carboxylic/amide spectral region were found despite the use of [2,5-$^{13}C_2$] glucose and the high magnetic field strength of 11.7 Tesla. As shown by Li et al (2008), the

lipid signal at 172.5 ppm is confined to a very narrow spectral region and would not have presented any spectral interference if no spatial localization were used.

Upon intravenous administration of the highly specific GABA-transaminase inhibitor gabaculine, the most significant change in the spectral pattern of the carboxylic/amide spectral region shown in Figure 2 is the progressive increase in the intensity of GABA C1 at 182.3 ppm. Because gabaculine was administered 2.5 hours after infusion of 99% enriched [2,5-$^{13}C_2$]glucose, essentially all precursors of GABA (neuronal glutamate and glial glutamine) had been heavily labeled with ^{13}C before GABA-transaminase inhibition began. Therefore, the steady increase in GABA C1 apparent in Figure 2 bears some similarity to that observed in proton MRS without infusing ^{13}C labeled glucose. Notably, the chemical shift difference between GABA C1 and glutamate C5 singlets (38 Hz in chemical shift difference at 11.7 Tesla) is much larger than that between glutamate H4 and GABA H2 multiplets (25 Hz in chemical shift difference at 11.7 Tesla). Prior to isotope chase, the plasma fractional enrichment of [2,5-$^{13}C_2$]glucose was determined to be 94.0 ± 1.1% (mean ± SD, n = 5).

The spectra in Figure 3 were acquired during isotope chase using unlabeled glucose from the same animal used to produce Figure 1. Two hours after gabaculine administration, the infusate was switched from [2,5-$^{13}C_2$]glucose to natural abundance glucose. As expected, signals of glutamate C5 and C1, glutamine C5 and C1, and aspartate C4 and C1 gradually lost their intensity during the ^{13}C isotope chase period due to the tricarboxylic acid cycles and the glutamate-glutamine cycle.

The most striking observation from the isotope chase experiment was the slow change in the signal of GABA C1. After the isotope chase began, the continued increase in total GABA concentration prior to the chase period was largely offset by the loss in ^{13}C labels from GABA C1. As a result, the variations in the signal intensity of GABA C1 during the 4.4 hour chase period were relatively small. At the end of the chase period, the plasma fractional enrichment of [2,5-$^{13}C_2$]glucose was determined to be 1.4 ± 1.6% (mean ± SD, n = 5). GABA C1 was the only major signal remaining at the end of the isotope chase. Similar to GABA, and in contrast to glutamate and glutamine, the slowly turning over N-acetylaspartate C5 signal at 174.3 ppm also showed little changes in intensity during the isotope chase. Based on high-resolution in vitro NMR analysis of brain perchloric acid extracts, the end point [^{13}C]GABA C1 concentration was 4.5 ± 0.3 μmol/g (n = 5, mean ± SD), corresponding to an isotopic fractional enrichment of 49.7 ± 2.6% (n = 5, mean ± SD).

Using the in vivo GABA C1 signal at the end point of the chase experiment as the concentration reference, the in vivo concentrations of ^{13}C-labeled glutamate C5, glutamine C5, and GABA C1 at all time points were quantified. Figure 4 plots the change in the concentration of ^{13}C-labeled glutamate C5, glutamine C5, and GABA C1 due to gabaculine administration and isotope chase from all animals (n = 5).

Discussion

Previous studies from our laboratory showed that ^{13}C label incorporation into GABA C2 from [1-^{13}C]glucose or [1,6-$^{13}C_2$]glucose or [2-^{13}C]acetate could be detected in vivo in the rat brain. This was achieved by spectrally resolving the GABA H2 signal at 2.30 ppm from the dominant neighboring glutamate H4 signal at 2.34 ppm in the proton-observed ^{13}C-detected (POCE) spectra at 11.7 Tesla (Yang et al, 2005). The GABA C2 signal at 35.2 ppm could also be measured directly in the ^{13}C aliphatic spectral region when the intense subcutaneous lipid signals were suppressed using a combination of spatial localization and volume suppression techniques. Retraction of the scalp underneath the ^{13}C-surface coil was also useful in suppressing spectral interference from lipids when performing non-survival rodent

experiments. Although either direct ^{13}C excitation or heteronuclear polarization transfer techniques could be used to measure GABA C2 (e.g., Li et al, 2005; de Graaf et al, 2006), our previous work showed that it is possible to partially resolve GABA C1 from the neighboring glutamate C5 at 4.7 Tesla in the monkey brain (Li et al, 2007), suggesting that brain GABA C1 synthesis studies can be performed at higher field strength.

The results presented here build upon this previous work, and demonstrate that it is also feasible to study GABA synthesis and the effect of GABA transaminase inhibition in vivo in the rat brain at high magnetic fields, by monitoring ^{13}C label incorporation into spectrally resolved GABA C1 signal at 182.3 ppm from exogenous [2,5-$^{13}C_2$]glucose or [2-^{13}C]glucose.

This study used PRESS-type direct localization of carboxylic/amide ^{13}C signals. The small long-range proton-carbon scalar couplings prevent effective heteronuclear polarization (e.g., Shen et al, 1999; Li et al, 2005; Xu and Shen, 2006) or Hartmann-Hahn transfer (Choi et al, 2005). Because of the narrow spectral dispersion in the carboxylic/amide ^{13}C spectral region, ^{13}C localization error due to chemical shift dispersion is quite small, even at the high field strength of 11.7 Tesla employed here. The carboxylic/amide signals span from GABA C1 at 182.3 ppm to N-acetylaspartate C5 at 174.3 ppm or 1000.3 Hz at 11.7 Tesla, corresponding to a maximum localization error of ±0.07 mm. Because the ^{13}C carrier frequency was placed at ~180.4 ppm, the actual ^{13}C localization error for the signals of interest (glutamate C5, glutamine C5, and GABA C1) was only ~±0.03 mm. In addition, the lack of resolvable ^{13}C - ^{13}C isotopomers in the carboxylic/amide spectral region simplified the quantification procedure, because there were no ^{13}C isotopomer-specific proton T_1 saturation differences associated with detection of ^{13}C signals in the aliphatic spectral region using heteronuclear polarization transfer techniques. Phase distortions of ^{13}C isotopomers (Xu et al, 2006) caused by the spin-echo delay in heteronuclear polarization transfer techniques were also absent in the carboxylic/amide spectral region because only carboxylic/amide singlets were detected.

As noted in our previous work using monkeys (Li et al, 2007), the intrinsic detection sensitivity of carboxylic/amide ^{13}C signals is less than their counterparts in the aliphatic region because their T_1s are longer. One key motivation for measuring ^{13}C signals in carboxylic/amide region is the exciting prospect of integrating ^{13}C MRS into the framework of parallel imaging using multiple ^{13}C receiver coils and whole-brain low power proton decoupling. In this study, the broadband stochastic proton decoupling scheme for detecting the carboxylic/amide carbons in the rat brain was evaluated in vivo over a 14 dB range, corresponding to a γB_2 of approximately 250–1250 Hz calibrated at the center of the spectroscopy voxel. We found that the in vivo performance of the stochastic proton decoupling scheme was relatively insensitive to the range of decoupling power settings investigated; this finding is in keeping with Ernst's theory of stochastic decoupling (Ernst, 1966). Because of the lack of interference from the intense subcutaneous lipid signals dominating the aliphatic region, ^{13}C signals in the carboxylic/amide region could be measured by encoding spatial information using a combination of coil sensitivity profiles and gradients just as in the case of water imaging. Under such an approach, PRESS-, STEAM-, and ISIS-type localization or other outer volume suppression techniques required for most proton or ^{13}C single-voxel or chemical shift imaging experiments would not be needed. Using multiple receiver coils could also significantly increase detection sensitivity in regions close to the surface. Notably, the results of the current work suggest that it may be possible to study the incorporation of ^{13}C labels into spectrally resolved GABA C1 at high magnetic field strength using the parallel imaging strategy for ^{13}C MRS described above.

The extent of ^{13}C labeling of GABA after acute inhibition of GABA transaminase using gabaculine shown in Figures 2 and 4 is substantially greater than that found in our previous study using POCE (Yang et al, 2005). In that study, gabaculine was administered prior to the

start of [1-^{13}C]glucose infusion, and the ^{13}C fractional enrichment of GABA was found to be markedly lower than that of its metabolic precursors. At the end of approximately two hours of [1-^{13}C]glucose infusion, the fractional enrichment of GABA C2 was only 12 ± 2% (Yang et al, 2005), corresponding to ~24% if [1,6-$^{13}C_2$]glucose were used. In contrast, in the current study GABA-transaminase was inhibited after 2.5 hours of [2,5-$^{13}C_2$]glucose infusion. As shown in Figure 4, this pre-infusion of ^{13}C labels allowed glutamate and glutamine C5 to be labeled close to the maximum extent prior to GABA-transaminase inhibition. Pre-labeling of the metabolic precursors of GABA forced de novo synthesized GABA to be largely ^{13}C labeled after administration of gabaculine. In the current study, the concentration of [1-^{13}C]GABA measured from Figure 4 is 3.5 ± 0.6 μmol/g (mean ± SD, n = 5), two hours after administration of gabaculine and continued [2,5-$^{13}C_2$]glucose infusion. The fractional enrichment of GABA C1 at this point was calculated to be ~83% using the previously measured rate of GABA pool size increase, which was obtained using the same acute gabaculine administration protocol (0.026 ± 0.004 μmol/g/min Yang et al, 2005).

Consistent with our earlier observations of markedly reduced ^{13}C label incorporation into GABA C2 from [1-^{13}C]glucose during acute GABA-T inhibition, our isotope chase experiment found that the loss of ^{13}C labels from GABA C1 was markedly slower than that from glutamate C5 and C1, glutamine C5 and C1, and aspartate C4 and C1. At the end of the 4.4 hour isotope chase, GABA C1 became the only dominant signal in the spectra. The glutamate, glutamine, and aspartate signals became less intense than, or comparable to, N-acetylaspartate C1, C4, and C5 signals.

After initiation of the isotope chase with unlabeled glucose, neuronal glutamate most rapidly loses its ^{13}C labels on glutamate C5 as a result of neuronal oxidative metabolism, which is unaltered by GABA-transaminase inhibition (Manor et al, 1996; Yang and Shen, 2005). Mainly through the glutamate-glutamine cycling flux between neurons and glia ($V_{glutamate\text{-}glutamine}$), neuronal glutamate is the major metabolic precursor for glial glutamine (Shen et al, 1999; Patel et al, 2001; 2005; Shen, 2006). As expected, in this study the rate of ^{13}C label loss from glutamine C5 during the isotope chase experiment was slower than glutamate C5. The slow loss of ^{13}C labels from GABA C1 observed in the isotope chase experiment was consistent with the notion that, under acute GABA-transaminase inhibition, the major metabolic precursor of GABA is astroglial glutamine (Patel et al, 2001; 2005). As such, the GABA-glutamine cycling flux ($V_{GABA\text{-}glutamine}$) was the primary mechanism responsible for replacing ^{13}C labels on GABA C1 with ^{12}C during the isotope chase period (Figs. 2 and 3). Because $V_{GABA\text{-}glutamine} \ll V_{glutamate\text{-}glutamine}$ (Yang et al, 2007), the rate of ^{13}C label loss from GABA C1 was, as expected, markedly slower than that from its major metabolic precursor astroglial glutamine.

Previous studies have suggested that intraterminal GABA concentration and its synthesis are regulated by product inhibition of GAD65 (Liden et al, 1987). In vitro, GABA has been found to be a competitive inhibitor of GAD and able to convert active holoenzymes into inactive apoenzymes (Martin and Rimvall, 1993). However, intracellular GABA concentrations are too low to regulate GAD in vivo (Neal and Shah, 1990; Martin and Rimvall, 1993). In addition, no evidence exists in the literature of short-term regulation of GAD by second messengers. The vast majority of the evidence has shown that GAD activity is not inhibited by its product, GABA (e.g., Neal and Shah, 1990; Yang and Shen, 2005; de Graaf et al, 2006). Nevertheless, the expression of GAD67 is thought to be regulated mainly by two mechanisms: (i) control of mRNA levels, and (ii) translation or protein stability. The latter mechanism is mediated by intracellular GABA concentrations (Rimvall and Martin, 1994; Sheikh and Martin, 1998). The down-regulation of GAD67 expression by increased GABA concentration has been confirmed experimentally by the use of chronic vigabatrin treatment, which (i) reduced GAD67 protein content (Rimvall and Martin, 1994; Sheikh and Martin, 1998); (ii) developed tolerance to

increased K^+-evoked GABA release from rat cerebral cortex (Neal and Shah, 1990); and (iii) reduced GABA synthesis rates (Manor et al, 1996). Because the duration of our experiment was relatively short, no significant change in GAD expression is expected. Therefore, the major contributor to the slow GABA synthesis observed after inhibition of GABA transaminase was expected to be the relatively small magnitude of $V_{GABA\text{-}glutamine}$.

In conclusion, we found that GABA metabolism can be studied in vivo by detecting the [^{13}C] GABA C1 signals in the carboxylic/amide spectral region where interference from subcutaneous lipids is absent. Broadband heteronuclear decoupling of the ^{13}C signals in the carboxylic/amide spectral region was achieved using stochastic waveforms with low radiofrequency power at very high magnetic fields. By pre-labeling the metabolic precursors of GABA and using isotope chase, we found that GABA synthesis was very slow accompanying the acute blockade of the GABA shunt by gabaculine. The slow synthesis of GABA after acute gabaculine administration was attributed to the small intercompartmental GABA-glutamine cycling flux between GABAergic neurons and astroglia. Because this study showed that using low power broadband stochastic proton decoupling is feasible even at very high field strength, it has important implications for the development of carboxylic/amide ^{13}C MRS methods to study brain metabolism and neurotransmission in human subjects at high magnetic fields (e.g., 7 or 11.7 Tesla).

Acknowledgments

The authors thank Dr. Steve Li for constructing the $^{13}C\{^1H\}$ RF coils/animal holder system, Dr. Steve Fox for performing the mass spectrometry analysis, Dr. Su Xu for preparing the figures, and Ms. Ioline Henter for editing the manuscript. This work was supported by the Intramural Program of NIH, NIMH.

References

Badar-Goffer RS, Bachelard HS, Morris PG. Cerebral metabolism of acetate and glucose studied by ^{13}C-n.m.r. spectroscopy. A technique for investigating metabolic compartmentation in the brain. Biochem J 1990;266:133–9. [PubMed: 1968742]

Behar KL, Boehm D. Measurement of GABA following GABA-transaminase inhibition by gabaculine: a ^{1}H and ^{31}P NMR spectroscopic study of rat brain in vivo. Magn Reson Med 1994;31:660–7. [PubMed: 7914662]

Blüml S, Moreno-Torres A, Shic F, Nguy CH, Ross BD. Tricarboxylic acid cycle of glia in the in vivo human brain. NMR Biomed 2002;15:1–5. [PubMed: 11840547]

Chapman AG, Evans MC. Cortical GABA turnover during bicuculline seizures in rats. J Neurochem 1983;41:886–9. [PubMed: 6875571]

Chen Z, Li SS, Yang J, Letizia D, Shen J. Measurement and automatic correction of high-order B_0 inhomogeneity in the rat brain at 11.7 Tesla. Magn Reson Imaging 2004;22:835–42. [PubMed: 15234452]

Choi IY, Lee SP, Shen J. Selective homonuclear Hartmann-Hahn transfer method for in vivo spectral editing in the human brain. Magn Reson Med 2005;53:503–10. [PubMed: 15723418]

De Belleroche JS, Bradford HF. Metabolism of beds of mammalian cortical synaptosomes: response to depolarizing influences. J Neurochem 1972;19:585–602. [PubMed: 5030976]

de Graaf RA, Patel AB, Rothman DL, Behar KL. Acute regulation of steady-state GABA levels following GABA-transaminase inhibition in rat cerebral cortex. Neurochem Int 2006;48:508–14. [PubMed: 16517019]

Ernst RR. Nuclear Magnetic Double Resonance with an incoherent radio-frequency field. J Chem Phys 1966;45:3845–3861.

Hassel B, Johannessen CU, Sonnewald U, Fonnum F. Quantification of the GABA shunt and the importance of the GABA shunt versus the 2-oxoglutarate dehydrogenase pathway in GABAergic neurons. J Neurochem 1998;71:1511–8. [PubMed: 9751184]

Hertz L. Functional interactions between neurons and astrocytes I. Turnover and metabolism of putative amino acid transmitters. Prog Neurobiol 1979 1979;13:277–323.

Kanamori K, Ross BD. The first in vivo observation of (13)C-(15)N coupling in mammalian brain. J Magn Reson 2001;153:193–202. [PubMed: 11740894]

Kanamori K, Ross DB. In vivo activity of glutaminase in the brain of hyperammonaemic rats measured by 15N nuclear magnetic resonance. Biochem J 1995;305:329–336. [PubMed: 7826349]

Kanamori K, Ross BD, Kuo EL. Dependence of in vivo glutamine synthetase activity on ammonia concentration in rat brain studied by 1H - 15N heteronuclear multiple-quantum coherence-transfer NMR. Biochem J 1995;311:681–688. [PubMed: 7487913]

Kanamori, K.; Ross, BD. In Vivo Nitrogen MRS Studies of Rat Brain Metabolism. In: Bachelard, Herman, editor. Advances in Neurochemistry. Vol. 8. Springer; New York: 1997.

Kaufman DL, Houser CR, Tobin AJ. Two forms of the gamma-aminobutyric acid synthetic enzyme glutamate decarboxylase have distinct intraneuronal distributions and cofactor interactions. J Neurochem 1991;56:720–3. [PubMed: 1988566]

Li S, Shen J. Integrated RF probe for in vivo multinuclear spectroscopy and functional imaging of rat brain using an 11.7 Tesla 89 mm bore vertical microimager. MAGMA 2005;18:119–27. [PubMed: 16007474]

Li S, Chen Z, Zhang Y, Lizak M, Bacher J, Innis RB, Shen J. In vivo single-shot, proton-localized ^{13}C MRS of rhesus monkey brain. NMR Biomed 2005;18:560–9. [PubMed: 16273509]

Li S, Yang J, Shen J. Novel strategy for cerebral ^{13}C MRS using very low RF power for proton decoupling. Magn Reson Med 2007;57:265–71. [PubMed: 17260369]

Li, S.; Wang, S.; Shen, J. Safety Evaluation for Proton Decoupled ^{13}C Spectroscopy at 3.0 T in Human Frontal Lobe: SAR Analysis Using Numerical Simulations. Proc Intl Soc Magn Reson Med, Abstract #783 and #1560; Toronto. 2008.

Li S, Zhang Y, Wang S, Yang J, Araneta MF, Farris A, Johnson C, Fox S, Innis R, Shen J. In vivo ^{13}C magnetic resonance spectroscopy of human brain on a clinical 3 Tesla scanner using [2-^{13}C]glucose infusion and low-power stochastic decoupling. Magn Reson Med. 2009in press

Lidén E, Karlsson L, Sellström A. Is the concentration of gamma-aminobutyric acid in the nerve terminal regulated via product inhibition of glutamic acid decarboxylase? Neurochem Res 1987;12:489–93. [PubMed: 3587508]

Lindgren S. Effects of GABAergic drugs on the GABA turnover in the substantia nigra and the corpus striatum of the rat. J Neural Transm 1987;69:33–46. [PubMed: 3035084]

Manor D, Rothman DL, Mason GF, Hyder F, Petroff OA, Behar KL. The rate of turnover of cortical GABA from [1-^{13}C]glucose is reduced in rats treated with the GABA-transaminase inhibitor vigabatrin (gamma-vinyl GABA). Neurochem Res 1996;21:1031–41. [PubMed: 8897466]

Martin DL, Rimvall K. Regulation of gamma-aminobutyric acid synthesis in the brain. J Neurochem 1993;60:395–407. [PubMed: 8419527]

Neal MJ, Shah MA. Development of tolerance to the effects of vigabatrin (gamma-vinyl-GABA) on GABA release from rat cerebral cortex, spinal cord and retina. Br J Pharmacol 1990;100:324–8. [PubMed: 2379037]

Patel AB, Rothman DL, Cline GW, Behar KL. Glutamine is the major precursor for GABA synthesis in rat neocortex in vivo following acute GABA-transaminase inhibition. Brain Res 2001;919:207–20. [PubMed: 11701133]

Patel AB, de Graaf RA, Mason GF, Rothman DL, Shulman RG, Behar KL. The contribution of GABA to glutamate/glutamine cycling and energy metabolism in the rat cortex in vivo. Proc Natl Acad Sci U S A 2005;102:5588–93. [PubMed: 15809416]

Patel AB, de Graaf RA, Martin DL, Battaglioli G, Behar KL. Evidence that GAD65 mediates increased GABA synthesis during intense neuronal activity in vivo. J Neurochem 2006;97:385–96. [PubMed: 16539672]

Paulsen R, Fonnum F. Comparison of results obtained with different methods for estimating GABA turnover in rat neostriatum. Biochem Pharmacol 1987;36:1539–44. [PubMed: 3555508]

Rimvall K, Martin DL. The level of GAD67 protein is highly sensitive to small increases in intraneuronal gamma-aminobutyric acid levels. J Neurochem 1994;62:1375–81. [PubMed: 8133268]

Sailasuta N, Robertson LW, Harris KC, Gropman AL, Allen PS, Ross BD. Clinical NOE 13C MRS for neuropsychiatric disorders of the frontal lobe. J Magn Reson 2008;195:219–25. [PubMed: 18829354]

Sailasuta, N.; Harris, K.; Abulseoud, O.; Ross, B. Cerebral glutamate metabolism via [2-^{13}C]glucose in normal brain. Proc Intl Soc Magn Reson Med, Abstract #2344; Honolulu. 2009.

Sheikh SN, Martin DL. Elevation of brain GABA levels with vigabatrin (gamma-vinylGABA) differentially affects GAD65 and GAD67 expression in various regions of rat brain. J Neurosci Res 1998;52:736–41. [PubMed: 9669322]

Shen J, Petersen KF, Behar KL, Brown P, Nixon TW, Mason GF, Petroff OA, Shulman GI, Shulman RG, Rothman DL. Determination of the rate of the glutamate/glutamine cycle in the human brain by in vivo ^{13}C NMR. Proc Natl Acad Sci U S A 1999;96:8235–40. [PubMed: 10393978]

Shen J. ^{13}C magnetic resonance spectroscopy studies of alterations in glutamate neurotransmission. Biol Psychiatry 2006;59:883–7. [PubMed: 16199016]

Slotboom J, Bovee WMMJ. A diabatic slice-selective rf pulses and a single-shot adiabatic localization pulse sequence. Concept Magn Reson 1995;7:193–217.

Sloviter RS, Dichter MA, Rachinsky TL, Dean E, Goodman JH, Sollas AL, Martin DL. Basal expression and induction of glutamate decarboxylase and GABA in excitatory granule cells of the rat and monkey hippocampal dentate gyrus. J Comp Neurol 1996;373:593–618. [PubMed: 8889946]

Tapia, R. γ-Aminobutyric acid metabolism and biochemistry of synaptic transmission. In: Lajtha, A., editor. Handbook of Neurochemistry. Vol. 3. New York: Plenum Press; 1983. p. 423-466.

Tunnicliff, G. 4-aminobutyrate transaminase. In: Boulton, AA.; Baker, GB.; Yu, PH., editors. Neurotransmitter Enzymes. Humana Press; 1986.

Xu S, Shen J. In vivo dynamic turnover of cerebral ^{13}C isotopomers from [U-^{13}C]glucose. J Magn Reson 2006;182:221–8. [PubMed: 16859940]

Yang J, Li CQ, Shen J. In vivo detection of cortical GABA turnover from intravenously infused [1-^{13}C] D-glucose. Magn Reson Med 2005;53:1258–67. [PubMed: 15906278]

Yang J, Shen J. In vivo evidence for reduced cortical glutamate-glutamine cycling in rats treated with the antidepressant/antipanic drug phenelzine. Neuroscience 2005;135:927–37. [PubMed: 16154287]

Yang J, Li SS, Bacher J, Shen J. Quantification of cortical GABA-glutamine cycling rate using in vivo magnetic resonance signal of [2-^{13}C]GABA derived from glia-specific substrate [2-^{13}C]acetate. Neurochem Int 2007;50:371–8. [PubMed: 17056156]

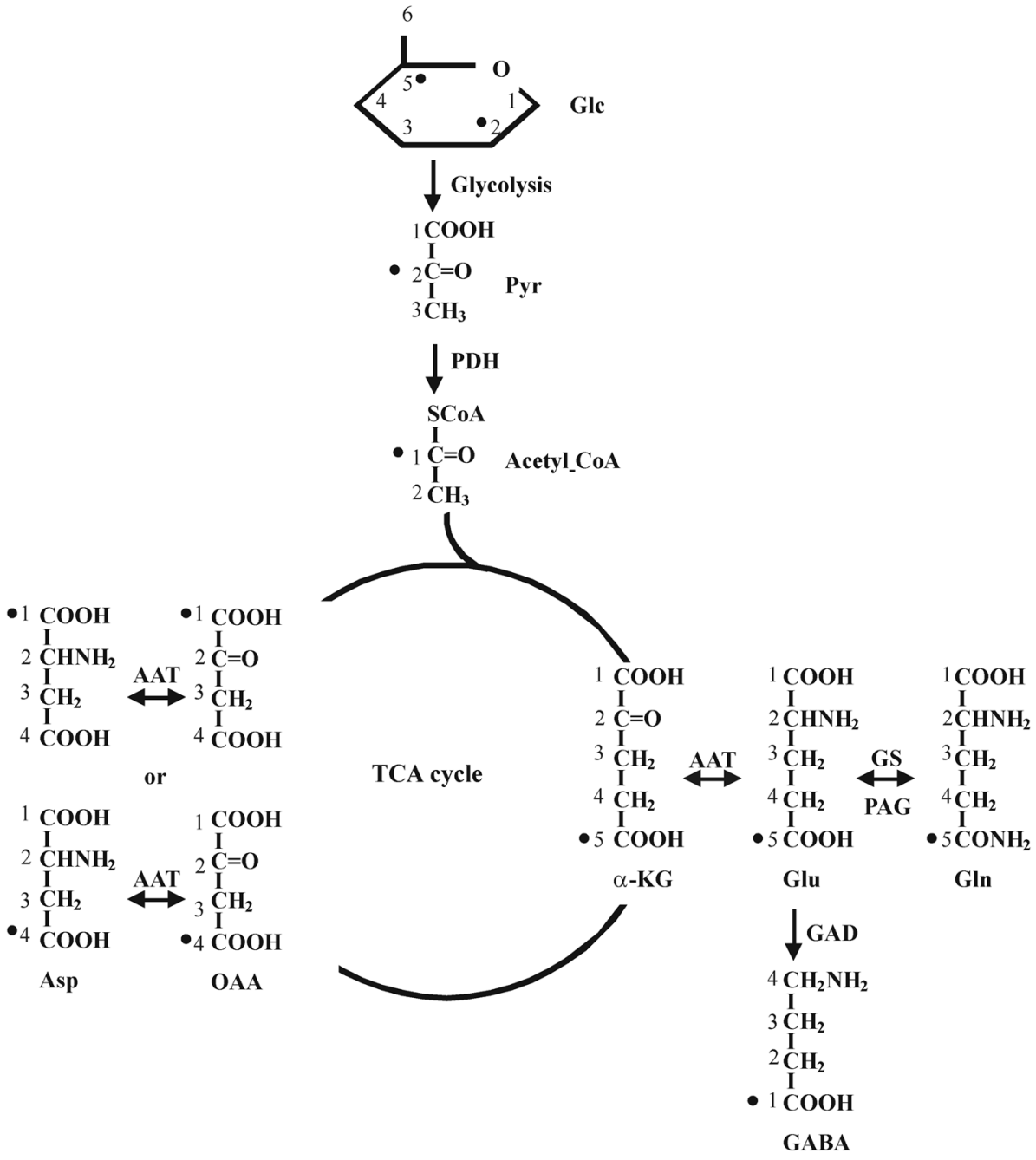

Fig. 1.

Schematic diagram of the label incorporation into glutamate, glutamine, aspartate and GABA from [2,5-$^{13}C_2$]glucose. Because both the turnover of glutamate C4 from [1,6-$^{13}C_2$]glucose and that of glutamate C5 from [2-$^{13}C_2$]glucose reflect the same de novo incorporation of exogenous ^{13}C labels into the TCA cycle (Li et al, 2007), only the first turn of the TCA cycle is drawn. ^{13}C labels originated from glucose C2 and C5 carbons are marked with •. Label scrambling during the first turn of the TCA cycle via symmetrical intermediates produces oxaloacetate with labels at C1 or C4. The carbons of glucose, pyruvate, acetyl CoA, α-ketoglutarate, glutamate, glutamine, GABA, oxaloacetate and aspartate are numbered. Abbreviations: AAT: aspartate aminotransferase; Asp: aspartate; GABA-T: GABA

transaminase; GAD: glutamic acid decarboxylase; Glc: glucose; Gln: glutamine; Glu: glutamate; GS: glutamine synthetase; α-KG: α-ketoglutarate; OAA: oxaloacetate; PDH: pyruvate dehydrogenase; Pyr: pyruvate.

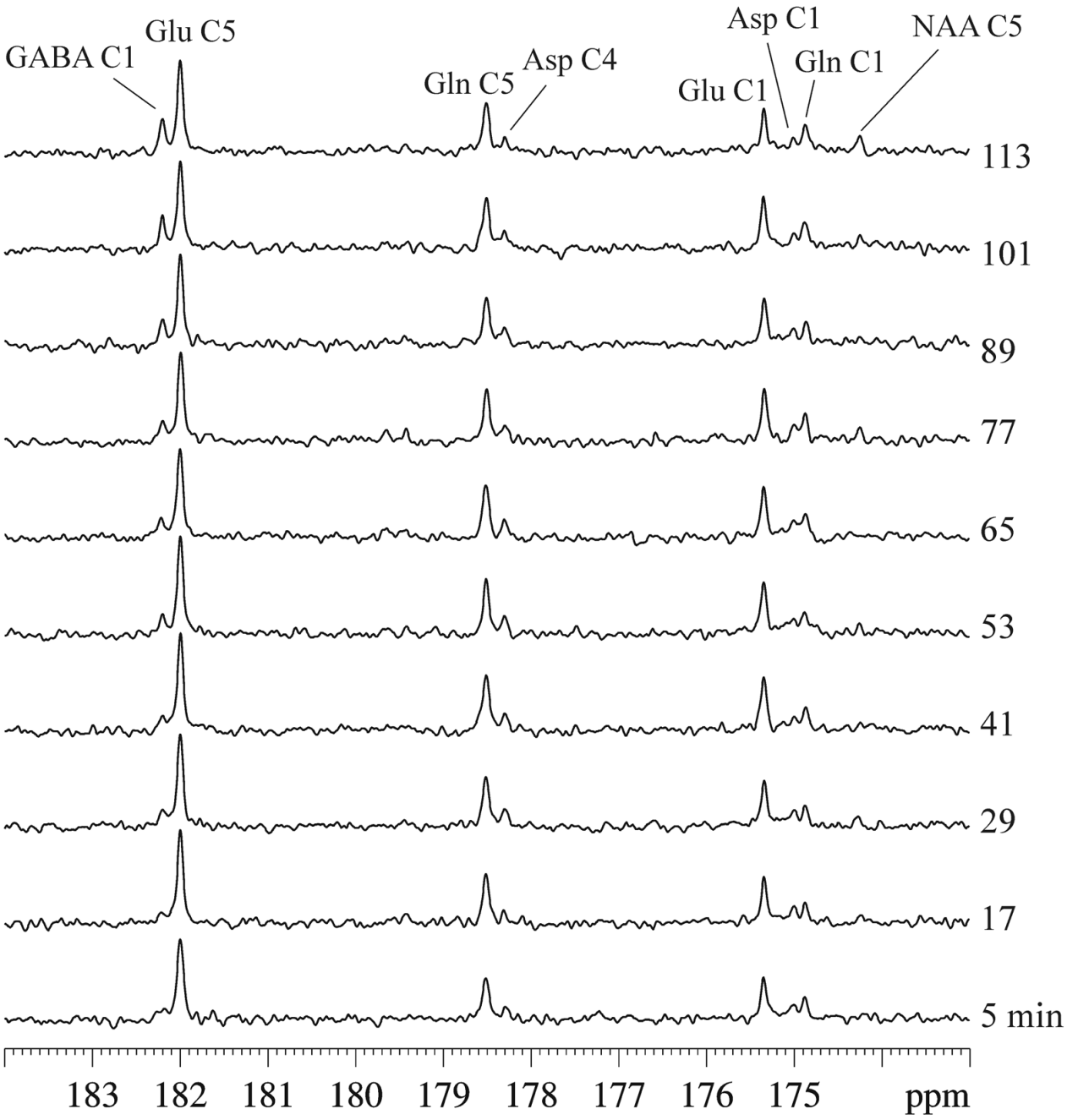

Fig. 2.

Typical in vivo ^{13}C spectra of GABA-transaminase inhibition during continuous infusion of [2,5-$^{13}C_2$]glucose acquired from an approximately 8.5 × 6 × 8.5 mm3 voxel in an individual rat (gb = 0.06, lb = −1. NS = 30 per spectrum with a total experimental time of ~2 hrs). The following signals were detected: glutamate C5 at 180.2 ppm, glutamine C5 at 178.5 ppm, GABA C1 at 182.3 ppm, aspartate C4 at 178.3 ppm, glutamate C1 at 175.4 ppm, glutamine C1 at 174.9 ppm, aspartate C1 at 175.0 ppm, and N-acetylaspartate C5 at 174.3 ppm. Bicarbonate signal was detected at 161.0 ppm (not shown for clarity). Glu: glutamate, Gln: glutamine, Asp: aspartate, NAA: N-acetylaspartate.

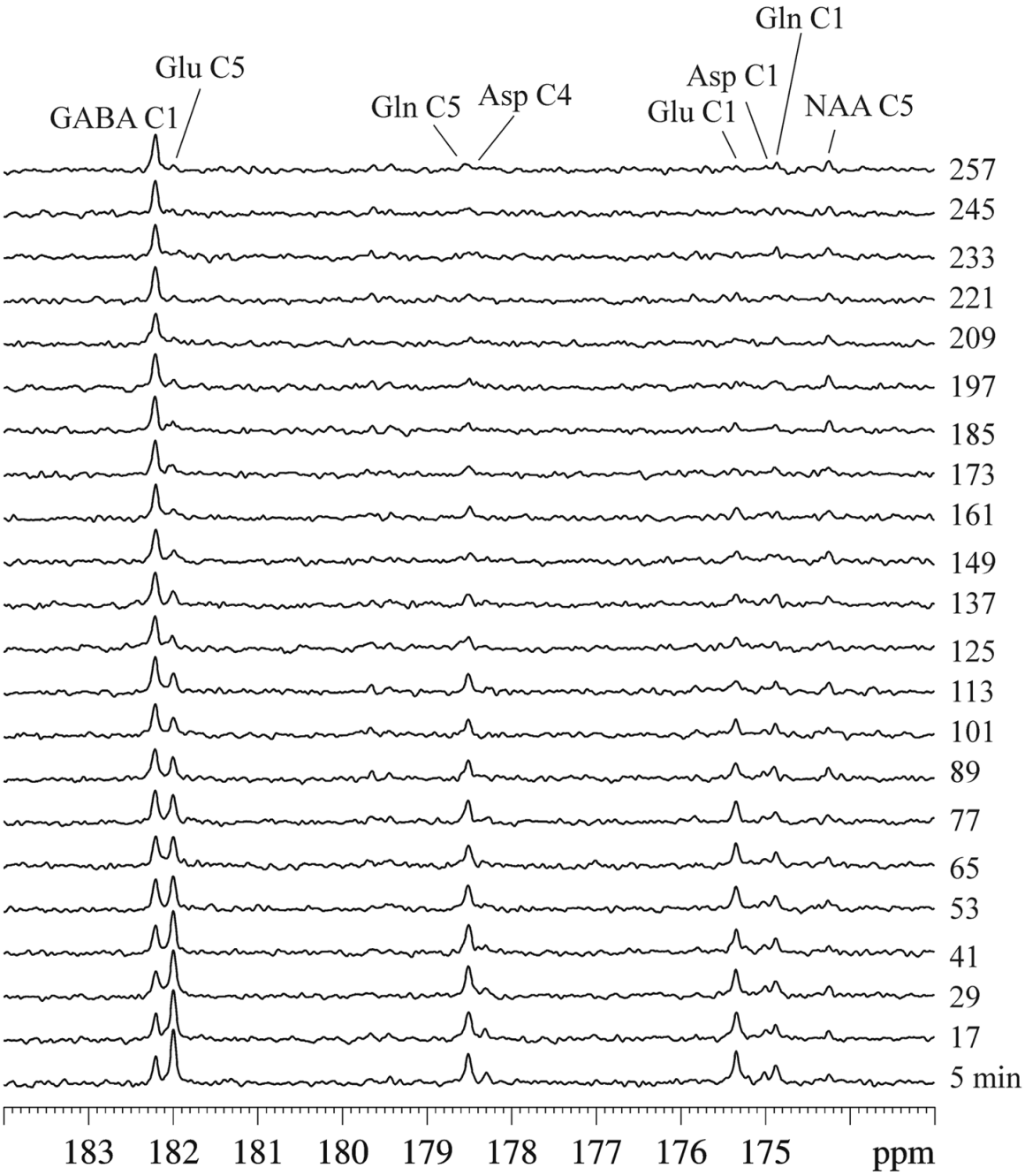

Fig. 3.

Typical in vivo ^{13}C spectra of acute GABA-transaminase inhibition during isotope chase using unlabeled glucose acquired from the same rat used for Figure 1. gb = 0.06, lb = −1. NS = 30 per spectrum with a total experimental time of 4.4 hrs. Signals of glutamate C5 and C1, glutamine C5 and C1, and aspartate C4 and C1 gradually lost their intensity during the chase period. Relatively small variations in the signal intensity of GABA C1 were seen. The slow turnover of the N-acetylaspartate C5 signal at 174.3 ppm also showed fewer changes in intensity during the isotope chase. Glu: glutamate, Gln: glutamine, Asp: aspartate, NAA: N-acetylaspartate.

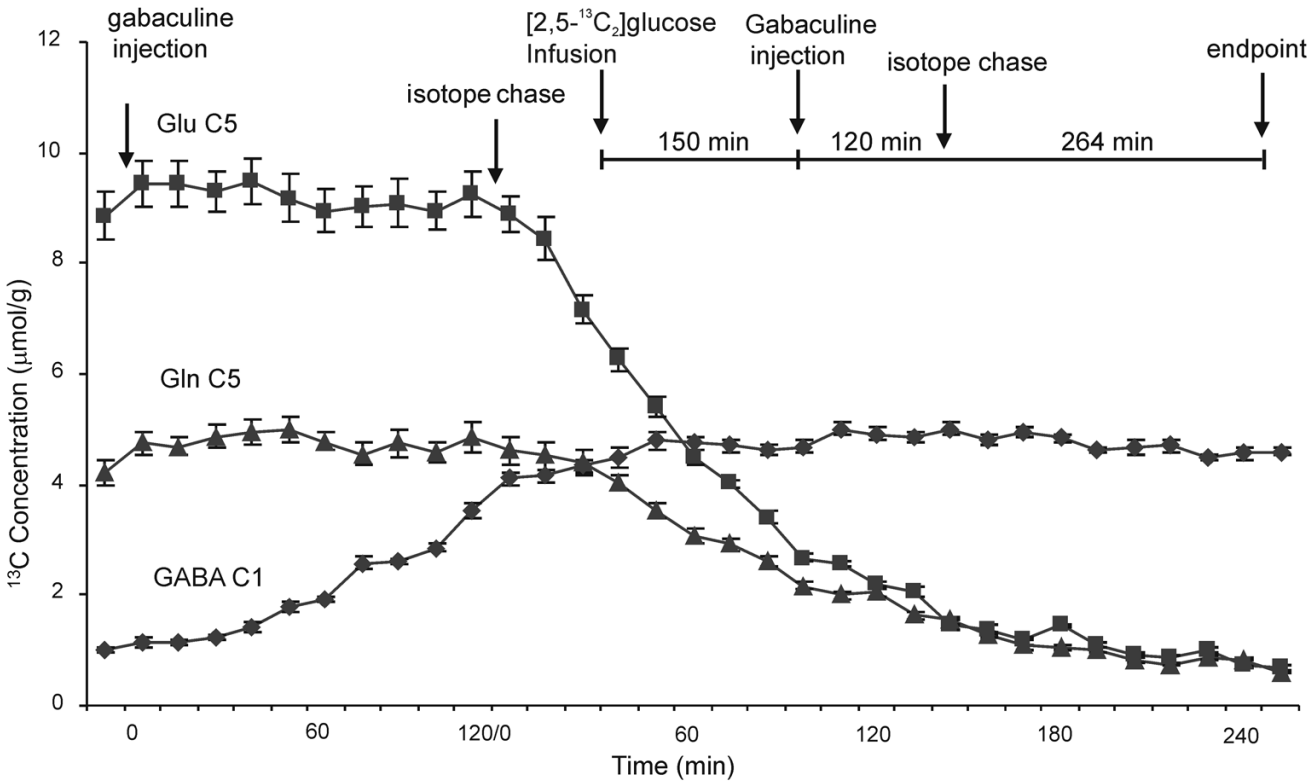

Fig. 4.

Time course of ^{13}C-labeled glutamate C5, glutamine C5, and GABA C1 concentrations (μmol/g) due to acute gabaculine administration and isotope chase by infusing unlabeled glucose. The inset depicts the treatment protocol starting with the initial 2.5 hr infusion of [2,5-$^{13}C_2$]glucose, followed by gabaculine administration and isotope chase 2 hr after gabaculine administration using natural abundance glucose. Quantification was based on high-resolution in vitro NMR analysis of brain perchloric acid extracts at the end point. The end point GABA C1 concentration was 4.5 ± 0.3 μmol/g (n = 5, mean ± SD), corresponding to an isotopic fractional enrichment of 49.7 ± 2.6% (n = 5, mean ± SD).